Seismic Analysis of Tensegrity Geodesic Domes Using the Force Density and Finite Element Methods

In this paper, we study the behaviour of tensegrity-type geodesic domes constructed from metallic alloys. This class of three-dimensional metallic structures is analysed under the combined action of seismic forces and gravity loads. The governing system of second-order differential equations, the solution of which provides the nodal displacement values, is solved through the combined application of the 'force density' and finite element methods. The results obtained by applying this integrated approach to two specific examples from the literature are comparable to those yielded by the conventional finite element method. For these specific tensegrity geodesic dome configurations, four distinct accelerograms are utilized. The solution of these problems demonstrates that the proposed method is superior because it provides immediate results, thereby eliminating the need for an iterative process based on successive incremental time steps. Furthermore, the obtained results are rigorously evaluated to verify the following: (a) whether the seismic excitation induces an increase in tensile stresses that exceeds the elastic limit, or whether it reduces the prestress in certain tension-only members—consequently indicating whether an increase in initial prestressing is required to ensure these elements remain in tension—and (b) whether any of the compression members (struts) are susceptible to buckling. Specifically, regarding the latter evaluation point, in cases where compressive forces induce buckling in the bars, structural redesign is necessary to successfully mitigate this phenomenon.

Keywords: *Tensegrity-type geodesic domes, combined application of the 'force density' and finite element methods, prestress in certain tension members, members (bars) under compression, buckling in certain compression members.*

Introduction

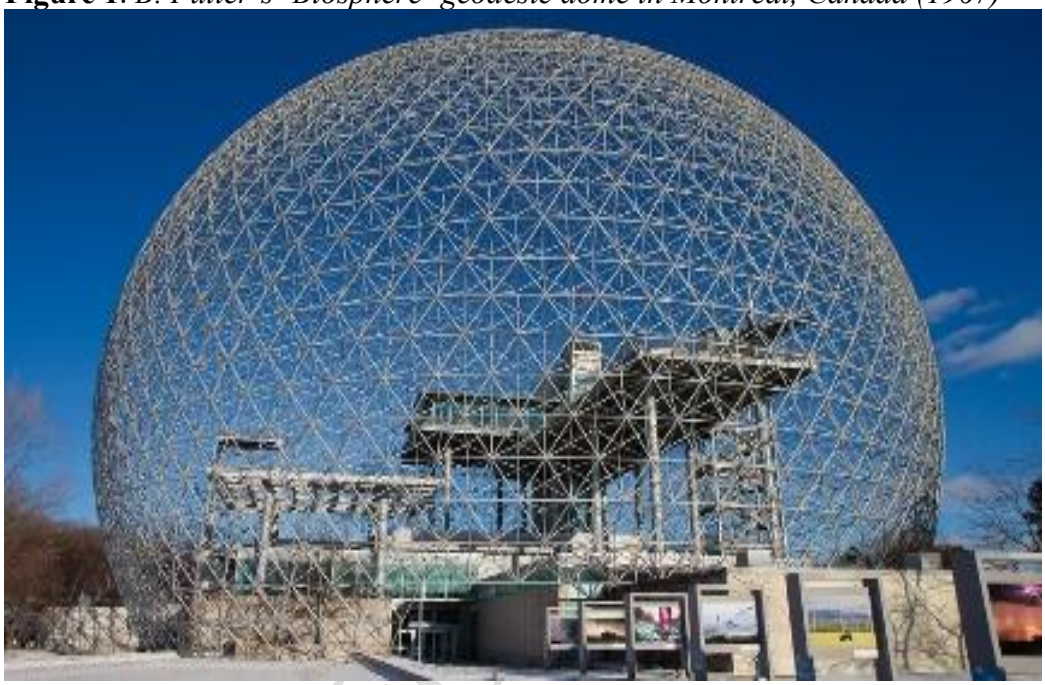
Geodesic domes are currently considered the most suitable structures for covering large spans. They comprise a network of compression members interconnected by tendons to form a three-dimensional grid, which typically constitutes a spherical truss of triangular configurations. Optimised material utilisation and lower capital costs, combined with the capacity to enclose exceptionally large areas, represent a distinct advantage of this specific structural typology over alternative metallic structures. The high stiffness of these three-dimensional systems accounts for their ability to span large distances using a minimal volume of structural material (e.g., geodesic domes manufactured from special alloys, aluminium, etc.).

Architects and engineers worldwide utilise a diverse range of connections for the components comprising this specific type of tensegrity dome, which is designed such that the tendons are under constant tension and the compression members are subjected to constant axial compressive force. The aesthetic value

ONLY FOR REVIEW

of geodesic domes is also highly significant, with their structural form constituting a prominent aspect of the architectural history of this type of gigantic tensegrity structures [1]. Notable examples include vaulted ceilings in buildings housing exhibition venues across North America and Europe, as well as natural rooflights designed by applying the bioclimatic residential architecture principles in certain regions of northern Europe.

Figure 1. *B. Fuller's 'Biosphere' geodesic dome in Montreal, Canada (1967)*



ONLY FO

Geodesic domes worldwide continue to inspire and impress both enthusiasts of modern architecture and curiosity-driven travellers. The elegant, aerodynamic profile of geodesic domes, the widespread availability of their constituent construction materials, and their inherent energy-efficient advantages create numerous opportunities to expand their implementation across various economic, professional, and social sectors. Since 1954, when Buckminster Fuller [1] patented the methods for discretising a sphere into spherical triangles (utilising an icosahedron as the initial solid element), geodesic steel-mesh domes have almost entirely superseded alternative typologies of large-span domes. In 1967, he presented the design configurations prepared for the impressive structure he later designated the 'Biosphere'—a dome with a diameter of 76 m built for the Expo 67 World's Fair in Montreal, Canada (Figure 1).

Fuller maintained that the geodesic dome represents nature's optimal structural form because, relative to alternative systems, it encloses the maximum volume utilising the minimum quantity of material. Harmonising with its surrounding environment, Fuller's dome relies entirely on its underlying circular geometry, eliminating the need for internal intermediate columns or load-bearing walls. Its primary structural advantage lies in minimizing the variety of component groups required for equal-length compression members. The largest

and most prominent geodesic dome projects globally include the Jeddah Superdome in Saudi Arabia, completed in 2021 (210 m in diameter), the Nagoya Dome, built in Nagoya, Japan, in 1997 (187 m in diameter), the Tacoma Dome in the US, constructed in 1983 (161 m in diameter), the Fukuoka Dome, built in Fukuoka, Japan, in 1993 (216 m in diameter), and the Superior Dome at Northern Michigan University in Marquette, completed in 1991, also in the US (163 m in diameter).

Sultan et al. [2] presented the results of a dynamic analysis of an existing lattice dome subjected to time-varying loads, whilst Masic et al. [3] provided a static analysis for designing domes with tension-only members. Although innovative configurations of tensegrity-type domes have been proposed by various researchers, studies examining geodesic domes under seismic loading remain scarce in the literature. Crucially, seismic actions rarely constitute the governing loading condition for geodesic domes, precisely owing to their characteristic low total mass relative to their enclosed volume. This explains the limited number of studies addressing the seismic response of geodesic domes; a notable exception is the work of Motro et al., which explores the dynamic characteristics of a cable (tendon) structure harmonically integrated within a metallic frame network [4]. The objective of that study was to determine the structural response under seismic excitation using matrix analysis alongside an iterative approach based on successive incremental time-steps (time-history analysis). These methodologies have been widely adopted to evaluate the response of existing structural systems under specific seismic excitations. Similarly, Kahla et al. [5] presented solutions for problems concerning existing domes and shell roofs deployed in various infrastructure projects.

Oppenheim and Williams [6] focused on methods for assessing structural responses under seismic loads for a three-dimensional metallic roof, while Masic and Skelton [7] evaluated the performance of lightweight structures exposed to earthquakes. Furthermore, the analysis of the dynamic stability of vaulted structures and their associated probabilities of failure under seismic action is featured in the work of several researchers. For instance, the concept of ‘stochastic seismic excitation’ is introduced in the study by Masic and Skelton. Most analyses concerning geodesic domes examine their fundamental form—the icosahedron—developed from Fuller’s original patent. However, Tan and Pellegrino [8] demonstrated that the octahedron might actually represent the optimal choice for constructing such domes instead of the icosahedron, owing to its superior load-distribution characteristics and seamless alignment with rectangular boundary foundations, though this alternative configuration introduces complications as it requires a greater quantity and variety of metallic elements.

This paper presents a numerical analysis of tensegrity-type geodesic domes subjected to seismic excitations utilising the ‘force density’ method ([9] and [10]), which falls within the category of Force Density Equilibrium Equation Methods (FDEEM). To date, research examining the seismic behaviour of tensegrity configurations has primarily focused on two-dimensional structures [11]. In this study, the developed space structures are generated based on the regular octahedron—a polyhedron that has not been extensively investigated in

ONLY FOR REVIEW

the literature thus far. These systems incorporate distinct component groups comprising cables [12] capable of developing tension-only forces, whilst the remaining groups function strictly as compression struts, thereby satisfying the fundamental definition of a tensegrity system. This specific class of geodesic dome is rigorously investigated herein.

It is worth noting that two distinct methodologies for subdividing spherical triangles, originally proposed by Fulinski [13] to design two geodesic domes subjected to seismic analysis, are examined. In this study, the identical geodesic domes evaluated by Fulinski are analysed by applying the FDEEM in conjunction with the Finite Element Method (FEM). Generally, the force density method is predominantly applied to non-linear problems where the primary objective is the form-finding of tension-dominated structures, such as membranes or cable networks, with the solution typically approached via successive linear approximations. Consequently, this method is uniquely suited to tensegrity-type geodesic domes rather than alternative structural typologies of geodesic configurations. The numerical analysis dictated by this methodology was executed under four distinct seismic excitations. The resulting data were compared with those derived from conventional FEM utilizing an incremental step-by-step procedure based on successive finite time-steps (time-history analysis). The outputs of the two methods are highly comparable; however, the FDEEM yields immediate results without requiring any iterative process.

The remainder of this paper is structured as follows: Section 2 outlines the mathematical formulations of the integrated application of the FDEEM and FEM. Section 3 demonstrates the application of this methodology to two geodesic domes subjected to four distinct seismic excitations. Finally, the results are compared with those derived from the conventional FEM, and concluding remarks are presented.

Integrated Force Density Equilibrium Equation Method (FDEEM) And Finite Element Method (FEM)

A fundamental concept concerning tensegrity structures is the term ‘force density’. For a member fabricated from a material that obeys Hooke's law, with nodal endpoints i and j, an initial length $L_{i,j}$, and an internal axial force $F_{i,j}$,, the ‘force density’ $q_{i,j}$ within the element is defined as follows (Figure 2):

$$q_{i,j} = \frac{F_{i,j}}{L_{i,j}} = (EA)_{i,j} \frac{\varepsilon^{(i,j)}}{L_{i,j}} \qquad (1)$$

where $\varepsilon^{(i,j)}$ is the strain, $(EA)_{i,j}$ represents the axial stiffness, E is the modulus of elasticity, and A denotes the cross-sectional area of the element [9]. This definition forms the basis of the numerical analysis presented herein. The ‘force density’ is assigned to a negative value when referencing a compressive force, and a positive value when referencing a tensile force.

ONLY FOR REVIEW

Figure 2. *Equilibrium of an interior node i of a two-dimensional tensegrity structure*

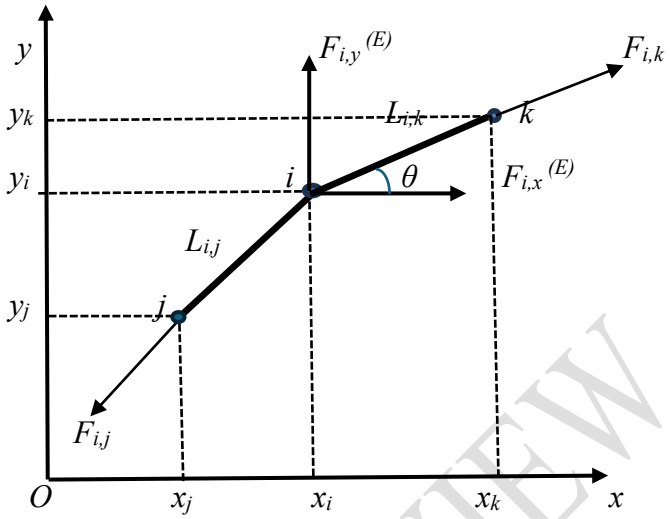


Figure 2 also illustrates the equilibrium of a typical interior node, *i*, which is located in the *Oxy* plane. This node is connected to nodes *j* and *k* by members of lengths $L_{i,j}$ and $L_{i,k}$., respectively. In the three-dimensional rectangular Cartesian coordinate system *Oxyz*, there are generally N_m nodes connected to the interior node *i* through N_m members. The equilibrium equations in the *Ox*, *Oy*, and *Oz* directions are as follows:

$$\sum_{j=1}^{N_m-N_p}\frac{x_i-x_j}{L_{i,j}}F_{i,j}=\sum_{j=1}^{N_m-N_p}\left(x_i-x_j\right)q_{i,j}=\sum_{j=1}^{N_m-N_p}q_{j,i}x_i-\sum_{j=1}^{N_m-N_p}q_{i,j}x_j=F_{i,x}^{(E)} \quad (2)$$

$$\sum_{j=1}^{N_m-N_p}\frac{y_i-y_j}{L_{i,j}}F_{i,j}=\sum_{j=1}^{N_m-N_p}\left(y_i-y_j\right)q_{i,j}=\sum_{j=1}^{N_m-N_p}q_{j,i}y_i-\sum_{j=1}^{N_m-N_p}q_{i,j}y_j=F_{i,y}^{(E)} \quad (3)$$

$$\sum_{j=1}^{N_m-N_p}\frac{z_i-z_j}{L_{i,j}}F_{i,j}=\sum_{j=1}^{N_m-N_p}\left(z_i-z_j\right)q_{i,j}=\sum_{j=1}^{N_m-N_p}q_{j,i}z_i-\sum_{j=1}^{N_m-N_p}q_{i,j}z_j=F_{i,z}^{(E)} \quad (4)$$

where $i = 1, \ldots, N$, and N is the total number of nodes in the structure. In equations (2) to (4), the left-hand sides contain the unknown 'force densities' $q_{i,j}$, whereas forces $F^{(E)}{}_{i,x}$, $F^{(E)}{}_{i,y}$, and $F^{(E)}{}_{i,z}$ represent internal forces that initially correspond to the prestress applied to specific tendons. Parameter N_p denotes the number of tendons connected to node *i* to which a prestress of a known magnitude is applied ($N_p \leq N_m$). The prestressing forces on the right-hand sides of equations (2) to (4) are expressed as follows:

$$F_{i,x}^{(E)}=-\sum_{j=1}^{N_p}\left(x_i-x_j\right)T_{i,j}, \qquad F_{i,y}^{(E)}=-\sum_{j=1}^{N_p}\left(y_i-y_j\right)T_{i,j},$$

$$F_{i,z}^{(E)}=-\sum_{j=1}^{N_p}\left(z_i-z_j\right)T_{i,j} \quad (5)$$

ONLY FOR REVIEW

where $T_{i,j}$ is the prestress per unit length of a member connecting nodes i and j. The study of the behaviour of a three-dimensional tensegrity structure is based on its equations of motion under forced vibration, which are given by [11]:

$$M_s \cdot \begin{bmatrix} \ddot{X} \\ \ddot{Y} \\ \ddot{Z} \end{bmatrix} + C_s \cdot \begin{bmatrix} \dot{X} \\ \dot{Y} \\ \dot{Z} \end{bmatrix} + K_s \cdot \begin{bmatrix} X \\ Y \\ Z \end{bmatrix} = \begin{bmatrix} F_x(t) \\ F_y(t) \\ F_z(t) \end{bmatrix} \tag{6}$$

where $\boldsymbol{M_s}$ is the global mass matrix, $\boldsymbol{C_s}$ the global damping matrix, and $\boldsymbol{K_s}$ the total stiffness matrix of the structure. Vectors $\boldsymbol{X(t)}$, $\boldsymbol{Y(t)}$ and $\boldsymbol{Z(t)}$ do not represent displacements; instead, they are the nodal coordinate vectors along the x, y and z directions, respectively, which are functions of time. Their introduction into the equations of motion (6) was performed using the definitions of the displacements $u_{i,x}$, $u_{i,y}$ and $u_{i,z}$ of node i, namely: $u_{i,x}=x_i(t+\delta t) - x_i(t)$, $u_{i,y}=y_i(t+\delta t) - y_i(t)$ and $u_{i,z}=z_i(t+\delta t) - z_i(t)$.

This change of variables was carried out to ensure compatibility with the concept of force density mentioned above. Furthermore, the total stiffness matrix $\boldsymbol{K_s}$ comprises two other global matrices [11]: the generalised Kirchhoff matrix, denoted by $\boldsymbol{D_{gl}}$, which contains the 'force densities' $q_{i,j}$ of the structural members and their combinations (arising from the applied prestressing forces $T_{i,j}$ in the tendons and the imposition of dead and live loads), and the conventional stiffness matrix $\boldsymbol{K_{FEM}}$, which is calculated via the FEM for small strains and displacements, namely:

$$K_s = D_{gl} + K^* \qquad D_{gl} = I_3 \otimes D, \qquad I_3 = \begin{bmatrix} 1 & 0 & 0 \\ 0 & 1 & 0 \\ 0 & 0 & 1 \end{bmatrix}, \qquad K^* = V^T \cdot K_{FEM} \cdot V, \tag{7}$$

where, in the expression above, $\boldsymbol{K^*}$ is the finite element stiffness matrix $\boldsymbol{K_{FEM}}$ after undergoing a reordering of rows and columns using the permutation matrix $\boldsymbol{V}$ to ensure compatibility in form with $\boldsymbol{D_{gl}}$. A similar reordering is performed on matrices $\boldsymbol{M_s}$ and $\boldsymbol{C_s}$.

From the above, it is evident that prior to assembling the global stiffness matrix $\boldsymbol{K_s}$, it is necessary to apply the FDEEM to calculate the 'force densities' $q_{i,j}$ within the structural members, which arise from the applied prestressing forces $T_{i,j}$ in the tendons. Solving this static problem before addressing the dynamic problem is crucial, as it incrementally leads to the computation of $\boldsymbol{D_{gl}}$. Consequently, the system of $3N$ linear equilibrium equations is solved; these equations represent an extension of equations (2) to (4) to the general case of a three-dimensional structure and take the following form:

$$\begin{bmatrix} D & O & O \\ O & D & O \\ O & O & D \end{bmatrix} \cdot \begin{bmatrix} x_c \\ y_c \\ z_c \end{bmatrix} = \begin{bmatrix} F_x^{(E)} \\ F_y^{(E)} \\ F_z^{(E)} \end{bmatrix} = \begin{bmatrix} \Psi_x^{(E)} \\ \Psi_y^{(E)} \\ \Psi_z^{(E)} \end{bmatrix} = \Psi^{(E)} \tag{8}$$

ONLY FOR REVIEW

where vector $\boldsymbol{\Psi}^{(E)}$ initially contains all known prestressing forces $T_{i,j}$ within the tendons and, in three-dimensional tensegrity structures, has dimensions $3N\times1$. The components of this vector are $\Psi_{i,x}^{(E)}$, $\Psi_{i,y}^{(E)}$ and $\Psi_{i,z}^{(E)}$, which share the same expressions as the components $F_{i,x}^{(E)}$, $F_{i,y}^{(E)}$ and $F_{i,z}^{(E)}$ in equations (5). Furthermore, matrix $\boldsymbol{D}$, known as the 'force density matrix' (FDM), relates the nodal coordinates to the forces acting upon them and is given by the relation:

$$D = P^T diag(q)\, P \tag{9}$$

In expression (9), elements $p_{a,c}$ of the connectivity matrix $\boldsymbol{P}$ take the following values:

$$p_{a,c} = \begin{cases} +1 & when\ c\ is\ the\ first\ joint\ of\ memeber\ a \\ -1 & when\ c\ is\ the\ second\ joint\ of\ memeber\ a \\ 0 & when\ c\ does\ not\ belong\ to\ memeber\ a \end{cases} \tag{10}$$

The system of equations (8) can be solved directly to yield the unknown values of the 'force densities' $q_{i,j}$ for structural configurations where the number of unknown 'force densities' at each node does not exceed two for a two-dimensional structure or three for a three-dimensional structure. However, when there are N_r redundant forces (degrees of static indeterminacy), Castigliano's second theorem [10] is employed to provide the additional N_r equations:

$$\frac{\partial U}{\partial Q^{(k)}} = \sum_{i=1}^{N_b} \frac{Q_i}{(EA)_i} \cdot \frac{\partial Q_i}{\partial Q^{(k)}} L_i = 0 \qquad k = 1,\cdots,N_r \tag{11}$$

where U is the total strain energy of the structure and N_b is the number of its members. Then, the internal forces Q_i are expressed as follows [9]:

$$Q_i = Q_i^{(RL)} + \sum_{j=1}^{N_r} Q_i^{(j)} Q^{(j)} \qquad i=1,\ldots,N \tag{12}$$

where $Q^{(j)}$ represents the unknown internal redundant forces. In relation (12), forces $Q_i^{(RL)}$ represent the axial forces acting on each of the members i, which are in equilibrium with all other actual loads (prestressing forces, gravity loads, and live loads) acting on the nodes. These forces are determined by removing the redundant structural components (members or supports) and solving the resulting statically determinate, stable structure—now referred to as the primary structure—under the action of the actual loads (prestressing). This solution yields the values of the forces $Q_i^{(RL)}$.

Furthermore, in equation (12), forces $Q_i^{(j)}$ represent the internal forces that are in static equilibrium and appear within the members of the primary structure (which at this stage is considered to be free from the actual applied prestressing load), when a unit load is applied sequentially to each redundant component. This implies that whenever a unit force is applied at the position of one redundant force, the force at the positions of the remaining redundant forces is zero. Since

ONLY FOR REVIEW

the redundant component is always an internal member (such as a strut, tendon, or cable), the unit force is applied as a pair of opposing collinear unit forces along the axis of the redundant member. Therefore, one pair of unit forces is applied at a time, and the primary structure is solved for each respective pair. Forces $Q_i^{(j)}$ are consequently dimensionless quantities, acting as the coefficients of $Q_i^{(j)}$, and their values constitute a set of statically admissible internal forces acting along the directions of the redundant forces. Consequently, the partial derivative of Q_i with respect to $Q^{(k)}$ in equation (11) takes the following form:

$$\frac{\partial Q_i}{\partial Q^{(k)}} = Q_i^{(k)} \quad k = 1, \cdots, N_r \qquad i = 1, \cdots, N_b \tag{13}$$

Substituting equations (12) and (13) into equations (11), the latter take the following form:

$$\sum_{i=1}^{N_b} \frac{Q_i^{(RL)} + \sum_{j=1}^{N_r} Q_i^{(j)} Q^{(j)}}{(EA)_i} \cdot Q_i^{(k)} L_i = 0 \qquad \text{or} \qquad \delta_k^{(RL)} + \sum_{j=1}^{N_r} h_{kj} Q^{(j)} = 0 \qquad k = 1, \cdots, N_r \tag{14}$$

where

$$\delta_k^{(RL)} = \sum_{i=1}^{N_b} \frac{Q_i^{(RL)} Q_i^{(k)}}{(EA)_i} L_i, \qquad h_{kj} = \sum_{i=1}^{N_b} \frac{Q_i^{(j)} Q_i^{(k)}}{(EA)_i} L_i \tag{15}$$

Equations (14), together with expressions (15), represent the additional equations being sought. It must be noted, however, that apart from prestressing, the tension members are also subjected to other types of loading.

Therefore, to account for all remaining loading types (gravity loads, live loads, and support reactions), a system of the form of equation (8) is solved, where the components $F_{i,x}^{(E)}$, $F_{i,y}^{(E)}$ and $F_{i,z}^{(E)}$ within the right-hand side (the load vector $\boldsymbol{\Psi}^{(E)}$) take the following form:

$$F_{i,x}^{(E)} = B_{i,x} + R_{i,x} \qquad F_{i,y}^{(E)} = B_{i,y} + R_{i,y}, \; F_{i,z}^{(E)} = -G_i - \frac{1}{2} \sum_{j=1}^{N_m} w_{i,j} L_{i,j} + B_{i,z} + R_{i,z} \tag{16}$$

where G_i is the self-weight of node i and $w_{i,j}$ is the weight per unit length of a member with end points at nodes i and j. Forces $B_{i,x}$, $B_{i,y}$ and $B_{i,z}$ are the concentrated live loads at the node, and $R_{i,x}$, $R_{i,y}$ and $R_{i,z}$ are the unknown support reactions (wherever a support exists) at node i. At each node and along each one of the three directions, there are also inertial and damping forces, which are incorporated into the mass and damping matrices, respectively, of equation (6). We assume that gravity loads act along the negative y-axis for two-dimensional structures, or along the negative z-axis for three-dimensional structures. Furthermore, we initially assume that the live loads and reactions act along the positive Ox, Oy, and Oz axes. If redundant members are present, Castigliano's

ONLY FOR REVIEW

theorem is applied as described above. The final values of $\boldsymbol{D_{gl}}$ are obtained through the superposition of the two solutions, namely, the solution of a problem considering the application of the prestressing forces in the tendons alone, and the solution of a problem in which only the application of gravity and live loads is considered. This means that the Principle of Superposition is applied due to the elastic behaviour of the material in the structure.

Thus, through the aforementioned procedure, the elements of the generalized matrix $\boldsymbol{D_{gl}}$ are calculated. By applying the methodology prescribed by the FEM, the elements of the stiffness matrix $\boldsymbol{K_{FEM}}$ are also computed, wherein an appropriate rearrangement of rows and columns is performed so that its form conforms to that of matrix $\boldsymbol{D_{gl}}$. Subsequently, the global stiffness matrix K_s is also calculated according to expression (7). Furthermore, the seismic ground accelerations α_g at the supports ultimately appear in the expressions of the known forces on the right-hand side of equations (6), alongside the remaining dynamic loadings. It remains, therefore, to modify the equations of motion (6) to account for the structural supports, which are either rigid or subject to a prescribed settlement. To this end, a rearrangement of the matrix elements is carried out via appropriate multiplications of $\boldsymbol{K_s}$ and $\boldsymbol{M_s}$ (damping $\boldsymbol{C_s}$ is conservatively neglected) with a predefined square Boolean matrix.

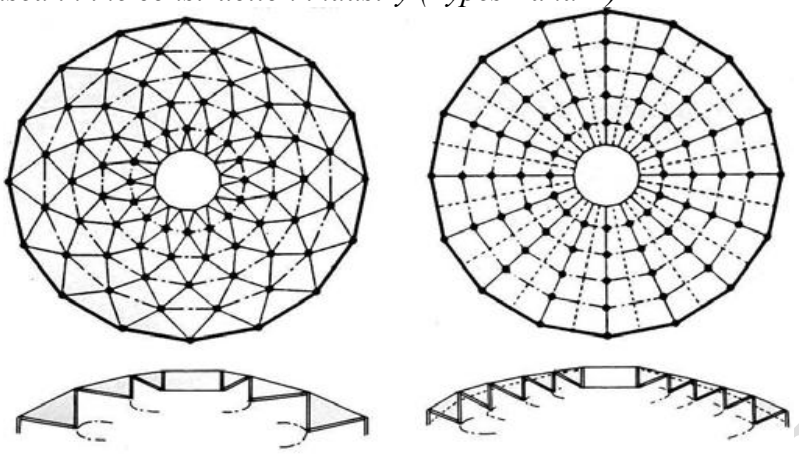
The solution of the system of differential equations (6) can be achieved after previously determining the mode shapes $\boldsymbol{\varphi_i}$ of the system and expressing the solution [*X, Y, Z*] as a superposition of the normal modes $\boldsymbol{\varphi_i}$ multiplied by appropriate coefficients $\boldsymbol{w_i(t)}$. By utilizing the orthogonality property of the normal modes, the decoupling of the functions within the equations is achieved, such that each equation contains only a single unknown function, which subsequently renders the solution of the system straightforward. This technique is known as ‘modal analysis’ (or ‘modal solution’) [12] and is successfully applied to tensegrity domes within the scope of this method. This is due to the capability for modal analysis that the method provides for this specific type of structure, which features tension-only members (cables) that are incapable of resisting compressive stress.

Numerical Results and Conclusions

The methodology presented above is applied to two geodesic domes subjected to four distinct seismic excitations: the Ancona earthquake (Italy), the Denizli earthquake (Turkey), the Friuli earthquake (Italy), and the Killini earthquake (Greece). All structural members of the geodesic domes are fabricated from high-strength, heat-treated aluminum alloy 6061, exhibiting high tensile and compressive strength (Figure 3).

ONLY FOR REVIEW

Figure 3. *Tensegrity geodesic domes of two different types which are widely used in the construction industry (Types I and II)*



I II

By applying the FDEEM, the values of the 'force densities' $q_{i,j}$ within the structural members are calculated, arising from the applied prestressing forces $T_{i,j}$ in the tendons, as well as the remaining forces acting on the structure described above. The computational results, along with the technical properties of the structural material, are presented in Table 1. Subsequently, the matrices $\boldsymbol{D_{gl}}$, $\boldsymbol{K_{FEM}}$ and $\boldsymbol{K_s}$, as well as $\boldsymbol{M_s}$ ($\boldsymbol{C_s}$ is omitted), are computed in the manner explained above, and system (6) is solved by applying the 'modal solution' technique. The maximum axial force values developed within the structural members are calculated and compared to those obtained from the FEM, utilising an iterative computation procedure based on successive finite time intervals (Time History) [13].

The two sets of results are comparable with each other (Table 1). However, the proposed method appears more advantageous as it yields direct results without the use of an iterative procedure. Furthermore, it requires a smaller number of numerical operations and less computer memory to construct the global stiffness matrix.

ONLY FOR REVIEW

Table 1. *Comparison of maximum absolute axial force values in members resulting from the application of the combined FDEEM and FEM and of the pure FEM (with application of an iterative procedure) [13]*

Nr	Type of earthquake	Young's Modulus of members (MPa) (GPa)	σ_y	Type of geodesic dome	Maximum axial force derived from FDEEM/FEM (kN)	Maximum axial force derived from FEM (Time History) [13] (kN)
1	Ancona seism	70	276	Geo. dome I	|-70.03|	|-69.54|
2	Ancona seism	70	276	Geo. DomeII	46.62	47.01
3	Denizil seism	70	276	Geo. Dome I	39.87	40.54
4	Denizil seism	70	276	Geo. DomeII	37.84	37.63
5	Friuli seism	70	276	Geo. dome I	12.61	12.82
6	Friuli seism	70	276	Geo. DomeII	13.45	13.31
7	Killini seism	70	276	Geo. Dome I	5.72	5.56
8	Killini seism	70	276	Geo. DomeII	|-6.32|	|-6.76|

The two sets of results are comparable (Table 1). However, the proposed method **is** more advantageous, as it yields direct results without the use of an iterative computational procedure. Also, it requires fewer numerical operations and less computer memory to construct the global stiffness matrix.

Furthermore, beyond the aforementioned scientific knowledge, a specific objective of the method is to achieve design safety; consequently, the results obtained are meticulously analysed to verify the following:

i. Whether the elastic limit is exceeded or the prestress is reduced. Additionally, whether an increase in the prestressing force of the tendons is required for them to remain in tension.
ii. Whether certain compression members (bars) fail due to exceeding the compressive strength limit or whether they undergo buckling.

The results are verified and do not exhibit any such exceedances or failures. Consequently, both types of geodesic dome under investigation, which are included in Reference [13], are safe against tension, compressive forces, and buckling phenomena. Thus, the present seismic analysis method complements existing wind action analysis methods, aiming to account for the broader potential of utilising this type of structure to cover large spans.

ONLY FOR REVIEW

References

Fuller RB. Synergetics: Explorations in the Geometry of Thinking. *Macmillan Publishing* 1975, New York, U.S.A.

Sultan C, Corless M, Skelton RE. Linear dynamics of tensegrity structures. *Engineering Structures* 2002; 24: 671-685.

Masic M, Skelton RE, Gill PE. Algebraic tensegrity form-finding. *International Journal of Solids and Structures* 2005*;* 42, no. 16-17: 4833-4858.

Motro R, Najari S, Jouanna P. Static and Dynamic Analysis of Tensegrity Systems. In: Proceeding of the ASCE International Symposium on Shells and Spatial Structure. Computational Aspects Lecture Note in Engineering 1986; 26: 270-279.

Kahla NB, Moussa B, Pons JC. Nonlinear dynamic analysis of tensegrity systems. *Journal of the International Association for Shell and Spatial Structures* 2000; 41: 49-58.

Oppenheim IJ, Williams WO. Vibration and damping in three-bar tensegrity structure. *Journal of Aerospace Engineering* 2001; 14: 85-91.

Masic M, Skelton RE. Selection of prestress for optimal dynamic/control performance of tensegrity structures. *International Journal of Solids and structures* 2008; 43: 2110-2125.

Tan GEB, Pelegrino S. Nonlinear vibration of cable-stiffened pantographic deployable structures. *Journal of Sound and Vibration* 2008; 314: 783-802.

Elliotis M, Christou P, Michael A. Analysis of Tensegrity Structures with Redundancies, by Implementing a Comprehensive Equilibrium Equations Method with Force Densities. *Advances in Numerical Analysis* 2016; 1: 1-12, http://dx.doi.org/10.1155/2016/4815289

Fung YC. Foundations of solid mechanics. *Prentice Hall*, *Inc.* 1977*,* New Jersey, U.S.A.

Feng X. Dynamic Response and Vibration Control of a Planar Tensegrity Beam under El Centro Seismic Excitation. *Journal of Aerospace Engineering and Mechanics* 2017; 1(2): 73–82.

J.T. Katsikadelis. Dynamic Analysis of Structures. *Symmetria Publications* 2012, Athens, Greece.

Pilarska D, Maleska T. Numerical Analysis of Steel Geodesic Dome under Seismic Excitations. *Materials* 2021; 14, 4493. https://doi.org/10.3390/ma14164493

ONLY FOR REVIEW